Adsorption Characteristics of *p*-Xylene-α,α′-dithiol on Gold and Silver Surfaces: Surface-Enhanced Raman Scattering and Ellipsometry Study

Sang Woo Joo, Sang Woo Han, and Kwan Kim*

Department of Chemistry and Center for Molecular Catalysis, Seoul National University, Seoul 151-742, Korea

Received: June 29, 1999; In Final Form: September 8, 1999

The adsorption behavior of *p*-xylene-α,α′-dithiol (*p*-XDT) on colloidal gold and silver surfaces has been investigated by means of surface-enhanced Raman scattering (SERS). *p*-XDT chemisorbed dissociatively on both the gold and silver surfaces but as mono- and dithiolate, respectively. Regardless of the bulk concentration of *p*-XDT, only a monolayer was assembled on the silver surface with a flat orientation by forming two Ag−S bonds. On the gold surface, the monothiolate species, *p*-XDT^{1-}, appeared to assume a rather flat orientation at a very low surface coverage, but as the surface coverage was increased, the adsorbate took a perpendicular orientation. Furthermore, when the bulk concentration of *p*-XDT was close to that required for a full-monolayer coverage limit, a band assignable to the S−S stretching vibration appeared at ∼509 cm^{-1} in the gold sol SER spectra. A separate ellipsometry measurement performed with vacuum-evaporated gold substrates revealed that up to trilayers could be assembled on gold in 1 mM *n*-hexane solution of *p*-XDT while only a monolayer formed in either methanol or ethanol solution. Although the exact causes were uncertain, such a difference in behavior seemed to have nothing to do with the oxygen species present in ethanol or methanol solution.

1. Introduction

In the past decade, self-assembled monolayers (SAMs) on metal surfaces have attracted tremendous research interest.[1] In addition to the fundamental interest in such metal adsorbate systems, practical considerations such as the modification of metal surfaces and the preparation of functional organic thin films have increased research activity in this area.[2,3] The most widely studied and well-characterized systems include alkanethiols, dialkyl sulfides, and dialkyl disulfides on gold and silver.[4−11]

Aliphatic as well as aromatic dithiols are known to adsorb on gold as monothiolates by forming one single Au−S covalent bond. The other thiol group is pendent with respect to the gold surface.[12−16] In contrast, dithiol molecules are usually adsorbed on silver as dithiolates by forming two Ag−S bonds.[14,17−19] The detailed origin of the different adsorption characteristics of dithiol molecules on gold and silver has not been fully clarified, however. Recently, Kohli et al.[13] reported the spontaneous organization of up to eight covalently attached layers formed on gold from solution-phase α,ω-dithiols, viz., 1,6-hexanedithiol, 1,8-octanedithiol, and 1,9-nonanedithiol. The multilayers were formed on gold by immersing the substrate in a 10 mM ethanol solution of the dithiol at 20 ± 1 °C for 12 h or in a 1 mM solution of the dithiol in *n*-hexane for 1 h at the same temperature. The linking chemistry between layers was claimed to be the oxidative formation of a sulfur−sulfur bond. However, in an investigation of the structure and photooxidation of 1,8-octanedithiol self-assembled on an evaporated gold film, Rieley et al.[15] interpreted its X-ray photoelectron spectrum, presuming that the adsorbate was present on gold as a monolayer with a structure in which one sulfur atom was bonded directly to the substrate at the Au/SAM interface, while the other was located remotely from the surface at the SAM/air interface. In their work, the self-assembly was performed in 2 mM ethanolic solution for 3 h. During the fabrication of CdS nanoparticulate layers on a SAM of 1,6-hexanedithiol or 1,10-decanedithiol on gold, Nakanishi et al.[16] claimed similarly that only a monolayer was formed when a gold substrate was immersed in 1 mM ethanolic solution of the dithiol for 12−24 h. On the other hand, Murty et al.[14] reported that a monolayer was exclusively formed on an evaporated gold substrate when *p*-xylene-α,α′-dithiol was self-assembled in 1 mM ethanolic solution overnight. The monolayer was nonetheless claimed to form disulfides upon exposure to thiols such as 4-methoxybenzenethiol, suggesting the formation of a prototypical bilayer. All of these data indicate that the adsorption characteristics of dithiols on gold are very dependent on the kind of solvent as well as the concentration and the duration of the self-assembly.

Guided by the above implications, we have examined the adsorption behavior of *p*-xylene-α,α′-dithiol (*p*-XDT) on gold and silver sol surfaces by means of surface-enhanced Raman scattering (SERS). We have already reported the SERS of *p*-XDT in an aqueous silver sol.[17] We have not examined, however, if there was a concentration effect. The main objective of this work is to ascertain whether the adsorbate structure is dependent on the surface coverage of *p*-XDT on both the gold and silver surfaces, by utilizing the fact that SERS provides high spectral resolution and sensitivity even for submonolayer adsorbates on Au and Ag surfaces.[20−22] For a more reliable analysis of SER spectra in gold sol, the feasibility of the formation of multilayers on the vacuum-evaporated gold was also examined by means of ellipsometry.

2. Experimental Section

2.1. Preparation of Ag and Au Sol. The method of preparation of the aqueous silver sol was reported previously.[23]

* To whom correspondence should be addressed. Phone: 82-2-8806651. Fax: 82-2-8743704. E-mail: kwankim@plaza.snu.ac.kr.

10.1021/jp992230+ CCC: $18.00
Published on Web 11/18/1999

Briefly, approximately 10 mL of 10^{-3} M $AgNO_3$ solution was added dropwise to 30 mL of 2×10^{-3} M $NaBH_4$ solution, which was chilled to ice temperature. The gold sol was prepared by following the recipes in the literature.[24] Namely, 133.5 mg of $KAuCl_4$ (Aldrich) was initially dissolved in 250 mL of water, and the solution was brought to boiling. A solution of 1% sodium citrate (25 mL) was then added to the $KAuCl_4$ solution under vigorous stirring, and boiling was continued for ca. 20 min. The resulting Ag and Au sol solutions were stable for several weeks. To 1 mL of Au or Ag sol solution, $10^{-3}-10^{-5}$ M methanolic solution of *p*-xylene-α,α′-dithiol (*p*-XDT, Aldrich) was added dropwise to a final concentration of 5×10^{-4} to 10^{-8} M by using a micropipet. The yellowish silver and purple gold sols became dark-blue and bluish-green, respectively, by the addition of *p*-XDT. All the chemicals otherwise specified were reagent grade, and triply distilled water of resistivity greater than 18.0 MΩ cm was used in making aqueous solutions.

2.2. Raman Spectral Measurements. Raman spectra were obtained using a Renishaw Raman system model 2000 spectrometer equipped with an integral microscope (Olympus BH2-UMA). The 514.5 nm radiation from a 20 mW air-cooled argon ion laser (Spectra Physics model 163-C4210) and the 632.8 nm from a 17 mW air-cooled He/Ne laser (Spectra Physics model 127) were used as the excitation sources for the Ag and Au sol SERS experiments, respectively. An appropriate holographic notch filter was set in the spectrometer, depending on the excitation source. Raman scattering was detected with 180° geometry using a Peltier cooled (−70 °C) CCD camera (400 × 600 pixels). A glass capillary (KIMAX-51) with an outer diameter of 1.5−1.8 mm was used as a sampling device. Data acquisition times used in the Ag and Au sol SERS experiments were 90 and 270 s, respectively. The holographic grating (1800 grooves/mm) and the slit allowed the spectral resolution to be 1 cm^{-1}. The Raman band of a silicon wafer at 520 cm^{-1} was used to calibrate the spectrometer, and the accuracy of the spectral measurement was estimated to be better than 1 cm^{-1}. The Raman spectrometer was interfaced with an IBM-compatible PC, and the spectral data were analyzed using Renishaw WiRE software, version 1.2, based on the GRAMS/32C suite program (Galatics).

2.3. Ellipsometry Measurements. Ellipsometric measurements were made for *p*-XDT layers self-assembled on gold substrates. Initially, gold substrates were prepared by resistive evaporation of titanium (Aldrich, >99.99%) and gold (Aldrich, >99.99%) at ∼10^{-6} Torr on batches of glass slides, cleaned previously by sequentially sonicating in ethanol, hot piranha solution (1:3 H_2O_2(30%)/H_2SO_4), and distilled deionized water. Titanium was deposited prior to gold to enhance adhesion of gold to the substrate. After the deposition of approximately 200 nm of gold, the evaporator was back-filled with nitrogen. The gold substrates were immersed subsequently into a solution of *p*-XDT. Various solvents, concentrations, and immersion times were adopted in this experiment. After the substrates were removed from the solution, they were rinsed with excess solvent and then dried in a N_2 gas stream. The ellipsometric thickness of such self-assembled *p*-XDT films was estimated using a Rudolph Auto EL II optical ellipsometer. The measurement was performed using the 632.8 nm line of a He/Ne laser incident upon the sample at 70°. The ellipsometric parameters, Δ and Ψ, were determined for both the bare clean substrate and the self-assembled film. The so-called DafIBM program supplied by the Rudolph Technologies was employed to determine the thickness values, assuming that the refractive index of the organic film was 1.45. At least four different sampling points were considered in order to obtain averaged thickness values.

TABLE 1: Spectral Data and Vibrational Assignments of *p*-XDT[a]

OR		SERS		
neat	anion	Ag sol	Au sol	assignment[b]
		In-Plane Modes		
3055			3048	2
1612	1611	1602	1608	8a
1574				8b
1511		1505	1511	19a
1320				3
1201	1201	1199	1203	7a
1182	1179	1176	1180	9a
1096				18b
745	752	743	741	1
638		630	635	6b
451		463		6a
		Out-of-Plane Modes		
977				17a
923				5
839		845	840	10a
556		551		16b
504		506		10b
		402		16a
213				11
		Substituent Modes		
2928		2926	2917	ν (CH_2 asym)
2840		2846		ν (CH_2 sym)
2553			2564	ν (SH)
1429		1417	1419	CH_2 (def)
1253			1252sh	CH_2 (wag)
1226	1234	1218	1221	CH_2 (wag)
793				CSH (bend)
788				CSH (bend)
675	695	645	663	ν (CS)
	681			ν (CS)
			509	ν (SS)
343		345	348	CCSH (tor)

[a] Units of cm^{-1}. [b] Made by referring to our previous report [ref 17].

2.4. Transmission Electron Microscope (TEM) Measurements. To estimate the sizes of gold and silver colloidal particles, their TEM images were obtained with a JEM-200CX transmission electron microscope at 200 kV after sequentially placing a drop of colloidal solution and a drop of methanol solution of *p*-XDT onto Ni/Cu grids.

3. Results and Discussion

3.1. Ordinary Raman Spectrum of *p*-XDT. Curves a and b of Figure 1 are the ordinary Raman (OR) spectra of *p*-XDT in neat solid state and in basic aqueous solution, respectively. Their peak positions are listed in Table 1 along with the appropriate vibrational assignments. The latter assignments are taken from our earlier report.[17] The bands in the two OR spectra could be correlated without difficulty except for the bands assignable to vibrations including SH groups. The band at 2553 cm^{-1} and the broad composite bands at 788 and 793 cm^{-1} in the OR spectrum of neat *p*-XDT, whose counterparts are completely absent in Figure 1b, are due to the SH stretching and the CSH bending vibrations, respectively.

3.2. SER Spectrum of *p*-XDT in Ag Sol. Figure 1c shows the SER spectrum of *p*-XDT in an aqueous silver sol. The concentration of *p*-XDT in aqueous silver sol, 10^{-6} M, is the same as that used in the previous report. As seen previously, *p*-XDT exhibited a strong enhancement of its Raman bands upon adsorption on the silver surface. The SER spectral pattern

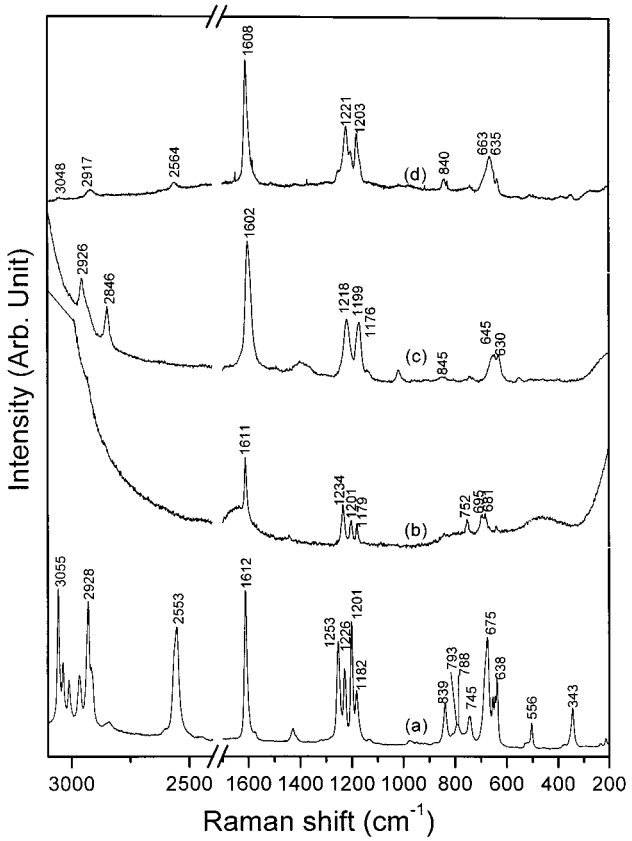

Figure 1. OR spectra of *p*-XDT (a) in neat solid state and (b) in basic aqueous solution. SER spectra of 10^{-6} M *p*-XDT (c) in aqueous silver sol and (d) in aqueous gold sol.

observed herein is little different from that in our previous report. To clarify the similarity and/or dissimilarity of the adsorption behavior of *p*-XDT on gold and silver surfaces, reproduction of the key points deducible from the analysis of the SER spectrum in an aqueous silver sol is needed. The peak positions of each band in the SER spectrum in Figure 1c and their correlation with the bands in the OR spectra are thus listed in Table 1. It is seen that the SH stretching and the CSH bending bands are completely absent in the SER spectrum, implying that *p*-XDT adsorbs on the silver surface after losing both of its thiol protons. We also note that the CS stretching vibration is substantially red-shifted in the SER spectrum. The counterpart of the CS stretching band at 675 cm^{-1} in Figure 1a, which has split into a pair of bands at 681 and 695 cm^{-1} in the dithiolate anion spectrum (Figure 1b), appears at 645 cm^{-1} in Figure 1c. The huge red shift of the CS stretching mode, as much as 50 cm^{-1}, can be taken as evidence for the participation of two sulfur atoms in surface binding. That is, electron donation from the sulfur atom to silver results in the weakening of the C−S bonds.[17] With the two sulfur atoms being coordinated to the silver surface, the benzene ring of adsorbed *p*-XDT will assume a flat stance with respect to the colloidal silver surface. This does not necessarily mean that the benzene ring also interacts directly with the silver surface. Nonetheless, considering that the bandwidths of the benzene ring modes such as ν_{10a}, ν_{9a}, and ν_{8a} at 839, 1182, and 1612 cm^{-1}, respectively, in Figure 1a have increased by 5−10 cm^{-1} upon surface adsorption, the possibility of direct interaction between the benzene ring and the surface seems to be very high.[25] Since the peak shift and band broadening of the ring modes are not as dramatic as those of the CS stretching mode, the chemisorption of *p*-XDT on silver is supposed to occur mainly via its two sulfur atoms.

According to the TEM measurement, the average diameter of the silver particle was 10 nm. Assuming that each ion of *p*-XDT^{2-} occupies an area of 0.58 nm^2 with a flat orientation on silver, the concentration of *p*-XDT required for the monolayer coverage is estimated to be 3.3×10^{-6} M.[26] This may suggest that the SER spectrum shown in Figure 1c corresponds to *p*-XDT^{2-} on silver in a submonolayer coverage. On these grounds, we have attempted to determine whether the adsorption characteristics of *p*-XDT on silver is dependent on the surface coverage as well as whether there is a possibility of forming multilayers on silver at higher concentrations than 3.3×10^{-6} M. Although not shown here, the SER spectral pattern was insensitive to the variation of the concentration of *p*-XDT in aqueous silver sol. The peak positions as well as the relative peak intensities were almost invariant in all SER spectra taken in various concentrations ranging from 10^{-8} to 5×10^{-4} M. Neither the SH stretching nor the CSH bending bands were identified. These indicate that, on one hand, *p*-XDT adsorbs on the colloidal silver surface as dithiolate at all concentrations assuming a flat orientation and, on the other hand, the possibility of the formation of multilayers is negligible (see Figure 3a, which depicts the adsorbed geometry of *p*-XDT^{2-} on silver).

3.3. SER Spectrum of *p*-XDT in Au Sol. Figure 1d shows the SER spectrum of *p*-XDT in an aqueous gold sol. In taking the spectrum, the concentration of *p*-XDT was 10^{-6} M. According to the TEM measurement, the average diameter of gold particles was 50 nm, so the concentration of *p*-XDT required for the monolayer coverage was estimated to be 9.0×10^{-6} M,[28] assuming that the adsorbate was oriented perpendicularly with respect to the colloidal gold surface (vide infra). This implies that the SER spectrum shown in Figure 1d corresponds to *p*-XDT on gold with a submonolayer coverage. On the other hand, the SER enhancement in gold sol in this work was substantially lower than that in silver sol. The enhancement factor in gold sol is intrinsically lower than that in silver sol,[29] and the lower enhancement in this work may have been caused by the gold particles being rather larger than is usually the case, i.e., 15 nm.[30]

The positions of SER peaks in Figure 1d are also listed in Table 1. It is clearly seen that the SER spectral pattern in gold sol is different from that in silver sol. The most noteworthy point is that a peak attributable to the SH stretching vibration is identified at 2564 cm^{-1} in Figure 1d. Although the CSH bending band could not be identified clearly, the appearance of the SH stretching band suggests that the adsorption behavior of *p*-XDT on gold is in obvious contrast with that on silver. Since the pH of the gold sol was ∼3, any pendent thiol group should be present as −SH without deprotonation. The other noteworthy point is that in Figure 1d the benzene ring CH stretching band is identified at 3048 cm^{-1}. Such a band was completely absent in the SER spectrum taken in silver sol. It has been well documented in the literature that the presence of the ring CH stretching band in an SER spectrum is indicative of a vertical (or at least tilted) orientation of the benzene ring moiety on a metal substrate.[31,32] The absence of the band in the SER spectrum in silver sol is consonant with the flat orientation of *p*-XDT^{2-} on silver. The presence of the SH stretching as well as the ring CH stretching bands in Figure 1d indicates that *p*-XDT should adsorb on gold as monothiolate with one of the two SH groups being pendent with respect to the gold surface. That is, one Au−S bond is formed, in contrast with the case of silver where two metal−sulfur bonds are formed. Much the same conclusion was made by Murty et al.[14] in the analysis of the SER spectrum of *p*-XDT on a vacuum-evaporated gold film.

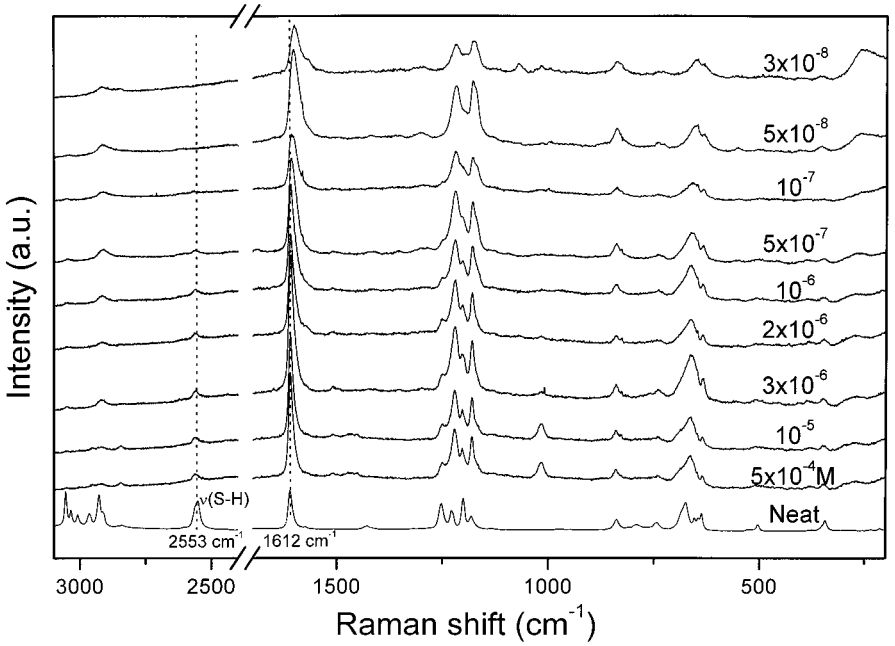

Figure 2. SER spectra of *p*-XDT in aqueous gold sol at various concentrations from 3×10^{-8} to 5×10^{-4} M in the region 3100−200 cm^{-1}.

Although identified at 2564 cm^{-1}, the SH stretching peak is not at all intense in Figure 1d. This may be indicative of a rather parallel orientation of the pendent S−H bond with respect to the gold sol surface. The low intensity of the SH stretching band may also be associated with the large distance of the −SH moiety from the sol surface caused by the formation of multilayered *p*-XDT film (vide infra).

In Figure 1d, the most typical in-plane ring mode, ν_{8a}, is observed at 1608 cm^{-1}, which is 6 cm^{-1} higher than its counterpart in Figure 1c. On the other hand, the typical out-of-plane ring mode, ν_{10a}, is observed at 840 cm^{-1} in Figure 1d, in contrast with its counterpart at 845 cm^{-1} in Figure 1c. These observations may be attributed to the fact that the adsorbate structure on gold is different from that on silver. The ν_{8a} mode may appear at a higher position in Figure 1d than in Figure 1c owing to the infeasiblity of the ring−surface π overlap on gold.[25] It is also noted that the amount of red shift of the CS stretching peak in Figure 1d with respect to the band in the dithiolate anion spectrum is far less than that in Figure 1c. In the dianion OR spectrum, two peaks appeared at 695 and 681 cm^{-1}, but in the gold sol SER spectrum, one peak appeared at 663 cm^{-1} while its counterpart appeared at 645 cm^{-1} in the silver sol SER spectrum. This may be understood by recalling that one sulfur atom participates in surface binding on the gold surface while two sulfur atoms take part in surface binding on the silver surface. The amount of electron donation from sulfur to metal should then be less on gold than on silver. It is intriguing that the SH stretching frequency in Figure 1d is 11 cm^{-1} higher than that in Figure 1a, i.e., in the neat OR spectrum. This upshift may indicate that the pendent, terminal SH group of *p*-XDT^{-1} on gold is free of any intermolecular hydrogen bonding.

An attempt was made to ascertain whether the adsorption characteristics of *p*-XDT on gold is dependent on the surface coverage. Figure 2 shows the SER spectra of *p*-XDT taken in gold sol with various concentrations of *p*-XDT from 3×10^{-8} to 5×10^{-4} M. It is remarkable that a very distinct SER spectrum can be obtained even at $\sim 10^{-8}$ M of *p*-XDT; for instance, see the peak at 1602 cm^{-1} at 3×10^{-8} M. Unlike with silver sol, the SER spectral pattern is seen, however, to be dependent on the bulk concentration of *p*-XDT in gold sol. In the SER spectrum taken at 10^{-7} M, the SH stretching band is clearly identified at $\sim$2560 cm^{-1}. Upon an increase in the bulk concentration of *p*-XDT, its intensity reached a plateau at $>3 \times 10^{-6}$ M. At $<10^{-7}$ M, however, the SH stretching band was vaguely observed, although other bands such as ν_{8a} were clearly identified in the SER spectrum. At $<10^{-7}$ M, the ring CH stretching was also hardly detectable in the SER spectrum. On the other hand, the CS stretching band was seen at 654 cm^{-1} at $\sim 10^{-8}$ M but at 663 cm^{-1} at $>10^{-6}$ M in Figure 2. The former peak position is closer than the latter to what is seen in the Ag sol SER spectrum (645 cm^{-1}). Although the peak position was invariant, the out-of-plane ring mode, ν_{10a} at 840 cm^{-1}, appeared more distinctly upon a decrease in the bulk concentration of *p*-XDT. Another noteworthy point is that the position of the ν_{8a} band varied as a function of the bulk concentration of *p*-XDT in gold sol. For instance, the peak appeared at 1602 cm^{-1} at 3×10^{-8} M but at 1606 cm^{-1} at 5×10^{-7} M, at 1608 cm^{-1} at 10^{-6} M, and at 1609 cm^{-1} at $>2 \times 10^{-6}$ M. It is interesting that the position of the ν_{8a} band at 3×10^{-8} M in the gold sol is the same as that in the silver sol. In the silver sol, the peak was seen at 1602−1603 cm^{-1} in the entire concentration region, 10^{-8} to 5×10^{-4} M. Besides, the ν_{8a} band in the gold sol SER spectrum is broadened as the concentration of *p*-XDT decreases. In fact, the bandwidth of the ν_{8a} band at $\sim 10^{-8}$ M in gold sol was nearly the same as that in silver sol. On the other hand, the SER scattering intensity in the Au−S stretching region became intensified as the concentration of *p*-XDT was decreased. In the silver sol, a broad SER scattering was identified in the Ag−S stretching region at all concentrations of *p*-XDT. All of these observations suggest that the orientation of *p*-XDT on gold is dependent on the surface coverage. Namely, when the surface coverage is very low, the adsorbate seems to assume a rather flat orientation even though it takes on a perpendicular orientation as the surface coverage increases. It is unfortunate that the structural change cannot be analyzed more precisely from the concentration-dependent SER spectra, since a set of SERS selection rules established so far is much dependent on the specific enhancement mechanism. We have to mention, however, that the conclusion made herein through an analysis of a

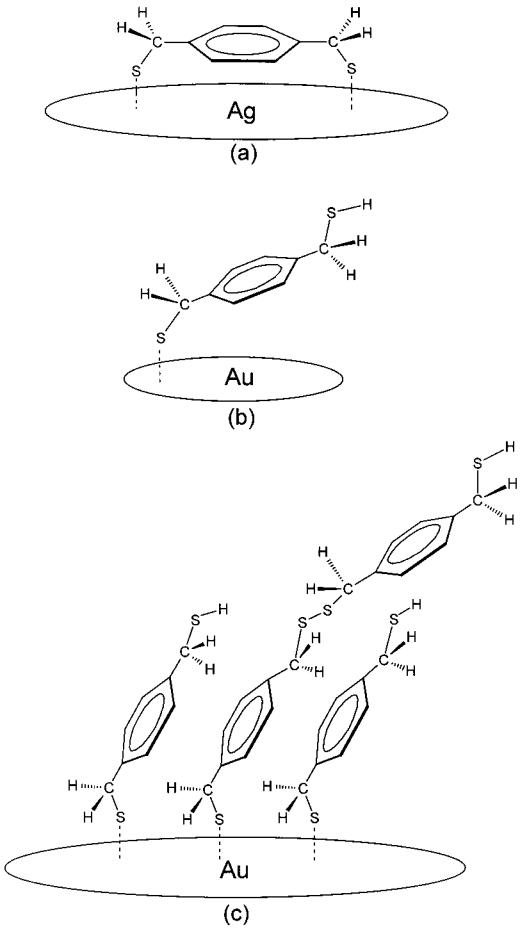

Figure 3. Plausible adsorbate structures of *p*-XDT (a) on silver and (b, c) on gold (b) at low surface coverage and (c) at high surface coverage.

few selected peak shifts and band broadening agrees, at least qualitatively, with the prediction based on the electromagnetic selection rule, that is, the orientation deducible from the presence and absence of the out-of-plane ring mode and the ring C−H stretching mode in the SER spectrum.[31−33] On these grounds, the plausible adsorbate structures of *p*-XDT on gold at low and high surface coverage limits are depicted in parts b and c of Figure 3, respectively. According to the discussion in section 3.4, the adsorbate was assumed to form multilayers at the high surface coverage limit. Nonetheless, it is not certain whether a coverage-dependent adsorbate structure is associated entirely with thermodynamics or due to the kinetics of self-assembly of *p*-XDT on gold. At low concentration, a flat geometry could be thermodynamically more stable because of the formation of two metal−sulfur bonds. However, as the concentration increases, an upright geometry would be more favorable, since the self-assembly should occur more quickly at higher concentration.

It has been well documented in the literature that for a SAM of short *n*-alkanethiol ($CH_3(CH_2)_nSH$, $n \leq 12$) on gold the alkyl chain is more disordered with lower packing densities.[34] It was also reported that the relative SER peak intensities of the symmetric and antisymmetric stretching modes of the CH_2 group could be associated with the ordering of those SAMs.[35,36] Although the same argument might not be applied to the SERS of *p*-XDT, the symmetric stretching band of the CH_2 group appeared more distinctly in the SER spectrum upon an increase in the bulk concentration of *p*-XDT. In fact, the antisymmetric and symmetric CH_2 stretching bands were observed, respectively, at 2917 and 2845 cm^{-1} in the SER spectra taken at 10^{-7} to 5×10^{-4} M in Figure 2. However, the symmetric stretching band is as intense as the antisymmetric stretching band at $\geq 10^{-5}$ M while the former is obviously weaker than the latter at $< 10^{-5}$ M. This may suggest that *p*-XDT assumes a more ordered conformation on gold as the packing density increases.

3.4. Feasibility of Multilayer Formation of *p*-XDT on Gold. In the SER spectral study of *p*-XDT self-assembled on a vacuum-evaporated gold film, Murty et al.[14] claimed that *p*-XDT adsorbed on the gold surface as a single-layered monothiolate. The possibility of the formation of multilayers was presumed by them to be very low. It is conceivable that the formation of multilayers would be affected by the kind of solvent as well as the concentration of adsorbing species. Regarding this matter, it may be worthwhile to note that a peak is identified at 509 cm^{-1} when the bulk concentration of *p*-XDT is above $\sim 10^{-6}$ M in the Au sol SER spectrum; for a better comparison, the SER spectra taken at $\sim 10^{-7}$ and $\sim 10^{-6}$ M are reproduced in Figure 4. Although it is tempting to assign the band to the ring ν_{10b} mode that appears at 506 cm^{-1} in the Ag sol SER spectrum, we prefer to assign the band to the S−S stretching vibration, since, as can be seen in the inset of Figure 4, no peak is really identified around 510 cm^{-1} when the bulk concentration of *p*-XDT is lower than 10^{-7} M in the gold sol. This implies that multilayers of *p*-XDT may have formed, albeit not exclusively, on the gold sol surface via the formation of S−S linkages. We have to mention that any disulfide species was not detected from NMR and Raman spectroscopy for 1 M *p*-XDT in methanol or hexane left overnight under ambient conditions. Recalling then that the concentration of *p*-XDT required for the monolayer coverage is 9.0×10^{-6} M, the presence of the S−S stretching band in the SER spectrum taken at 10^{-6} M indicates that multilayers can be formed even at a submonolayer coverage limit. This implies that the adsorption of *p*-XDT on the colloidal gold surface does not take place homogeneously from the early stages of adsorption.

The SER band at 509 cm^{-1} in Figure 4, attributed above to the S−S stretching vibration, is weaker by a factor of ~25 than the S−S stretching band at 505 cm^{-1} in the OR spectrum of neat dibenzyl disulfide when their intensities are normalized with respect to the ring ν_{8a} bands at 1600 cm^{-1}. (The present comparison may be somewhat irrational, since we have not taken into account that the ring ν_{8a} modes are usually more enhanced (about 10 times) than the substituent modes in the SER spectra. Even taking into account the latter effect, the SER band at 509 cm^{-1} is indeed weak.) The low intensity of the S−S stretching band in the SER spectrum of *p*-XDT may be due to imperfect multilayer coverage on the monolayer. On the other hand, on the basis of the electromagnetic enhancement mechanism, the low intensity of the S−S stretching band may be associated with the large distance of the −SS− moiety from the sol surface. Similarly, the SH stretching band might have appeared weak because of the formation of multilayered *p*-XDT film. In addition, the above bands would be weak, since the S−S and S−H bonds were all aligned quite parallel to the sol surface. Regarding these matters, we have to mention that a band is identified at ~500 cm^{-1}, as in the case of gold sol, when a SER spectrum is taken using an electrochemically roughened gold substrate after soaking in 1 mM *n*-hexane solution (data not shown). The peak was as weak as that in Figure 4. Considering then that a bi- or trilayered *p*-XDT film can be formed on a vacuum-evaporated gold substrate in 1 mM *n*-hexane solution (vide infra), the above reasoning on the low intensity of the SS stretaching band looks reasonable.

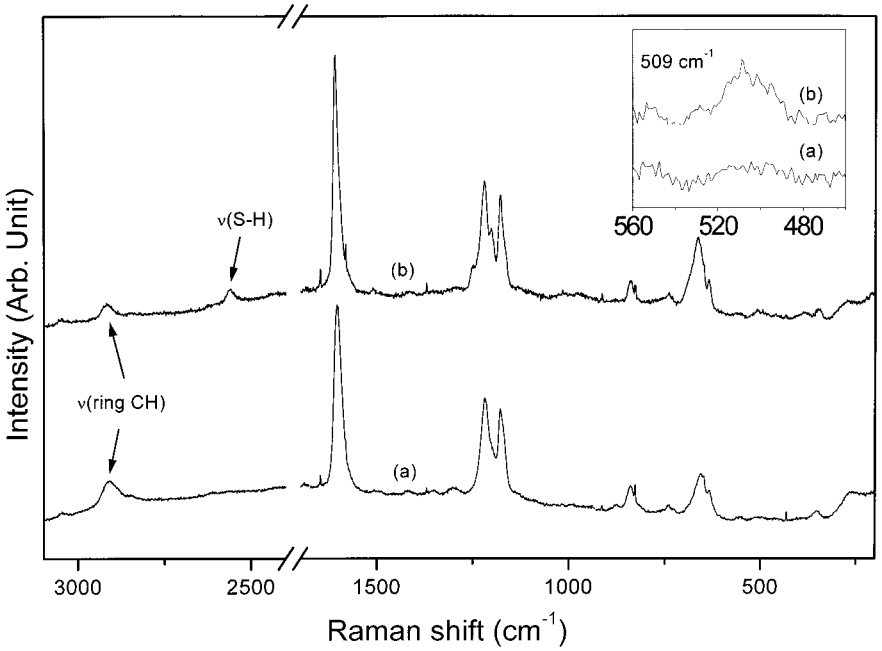

Figure 4. SER spectra taken (a) at a low bulk concentration ($\sim 10^{-7}$ M) and (b) at high concentration of *p*-XDT ($\sim 10^{-6}$ M) in gold sol. The inset is drawn to show more clearly the S−S stretching region.

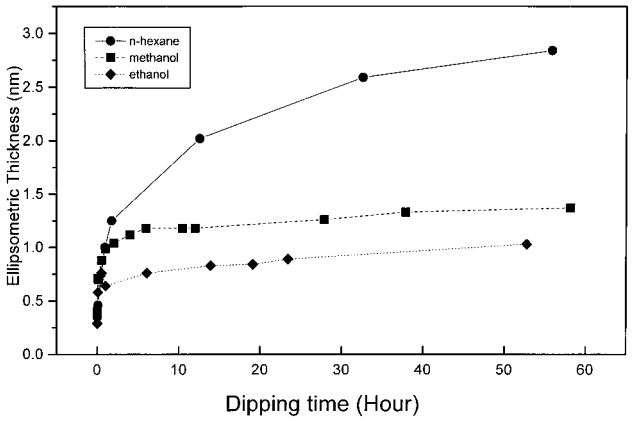

Figure 5. Ellipsometric thicknesses of *p*-XDT layers self-assembled on vacuum-evaporated gold substrates in 1 mM *p*-XDT solution in methanol, ethanol, and *n*-hexane for a duration of up to 60 h.

The feasibility of the formation of multilayers of *p*-XDT on the gold surface was further examined by measuring the ellipsometric thickness of *p*-XDT layers on vacuum-evaporated gold substrates. In Figure 5 are shown the ellipsometric thicknesses of *p*-XDT layers self-assembled on vacuum-evaporated gold substrates in 1 mM *p*-XDT solution in methanol, ethanol, and *n*-hexane. Even after taking account of the surface roughness factor for the vacuum-evaporated gold film ($\sim$1.3),[37] the 1 mM solution is thought to be concentrated enough for the formation of multilayers. It is seen that the thickness of the self-assembled layer is dependent on the kind of solvent. After prolonged immersion in 1 mM ethanol solution, the thickness of the *p*-XDT layer attained 0.8 nm while in methanol and *n*-hexane solutions the values were as large as 1.4 and 2.6 nm, respectively. (It has to be mentioned that even after a 60 h immersion we could not identify any disulfide in the solution phase using NMR and Raman spectroscopy.) Assuming that the monothiolate, *p*-XDT^{1-}, has a perpendicular orientation on the gold surface, the thickness of a full-covered *p*-XDT monolayer is estimated to be 1.14 nm, using the known bond lengths, bond angles, van der Waals atomic radii, and the approximate distance between the sulfur atom and the gold surface (0.15 nm).[38] Considering that benzylmercaptide on Au(111) has a perpendicular orientation with respect to the gold substrate,[39] it may not be unreasonable to assume that *p*-XDT^{1-} bound to gold via only one Au−S bond also has a perpendicular stance with respect to the underlying gold substrate. Although the present estimate is somewhat rough, it suggests that a near full-covered *p*-XDT monolayer is formed on the gold substrate in 1 mM methanol solution. In contrast, the measured ellipsometric thickness suggests that a bi- or trilayered *p*-XDT film is presumably formed in 1 mM *n*-hexane solution while only two-thirds of a layer is formed in 1 mM ethanol solution (vide supra). This difference would be associated with the greater solubility of oxygen in ethanol or methanol as suggested by Kohli et al.[13] Nonetheless, from a separate experiment multilayers did not seem to form even in the deaerated ethanol medium. Hence, other causes have to be searched out to elucidate the solvent dependence of the SAM formation.

To see the concentration effect on the final average thickness, *p*-XDT has also been self-assembled on a vacuum-evaporated gold substrate in 10^{-5} to 4×10^{-3} M methanol solution. After a 50 h self-assembly, the ellipsometric thicknesses were determined to be 1.1, 1.4, and 1.7 nm, respectively, when the self-assembly was performed in 10^{-5}, 10^{-4}, and 4×10^{-3} M solutions. This suggests that the surface coverage of *p*-XDT on gold should also depend on the concentration of the adsorbing molecules in the bulk medium. In a methanol medium, a near-full-covered *p*-XDT monolayer should assemble on gold in the concentration range 10^{-4}−10^{-3} M. This view is consonant with the report of Murty et al.[14] that they could not identify the presence of the S−S stretching band in the SER spectrum of *p*-XDT that had been self-assembled on gold overnight in 1 mM methanol solution. It is, however, intriguing that we could identify the S−S stretching band in the SERS of *p*-XDT in aqueous gold sol. Since the solubility of *p*-XDT in water was very low, we added a methanol solution of *p*-XDT to the Au sol solution to obtain the SER spectra. The present observation reveals that multilayers of *p*-XDT can be formed on the colloidal gold surface even in an aqueous methanol medium, albeit that

the formation of an intermolecular S−S bond is highly infeasible when *p*-XDT is self-assembled on a vacuum-evaporated gold film in <1 mM methanol solution. The exact cause of the difference is uncertain, but it may indicate that the adsorption characteristics are dependent on the detailed structure and morphology of metal surfaces.

4. Summary and Conclusion

We were able to confirm that *p*-XDT is adsorbed on gold as monothiolate by forming a single Au−S bond while it adsorbs on silver as dithiolate. The presence of the S−H stretching band in the SER spectrum in a gold sol indicated that one thiol group should be pendent with respect to the gold surface. From the concentration dependence study, it appeared, however, that the orientation of the adsorbed species is dependent on the surface coverage. Although the SER spectral pattern in a silver sol hardly changed upon variation of the bulk concentration of *p*-XDT, the qualitative SER spectral features in a gold sol suggested that the adsorbate should assume a rather flat orientation at a very low surface coverage, albeit that it took a perpendicular orientation at the higher surface coverage limit. Furthermore, the pendent SH group of *p*-XDT on gold was seen to react with free *p*-XDT molecules in the solution phase, resulting in the formation of disulfide multilayers. When the bulk concentration of *p*-XDT was somewhat close to that required for a full monolayer coverage limit, a band assignable to the S−S stretching vibration appeared at ∼509 cm^{-1} in the gold sol SER spectra. The possibility of multilayer formation on the gold surface was also confirmed by the self-assembly of *p*-XDT on vacuum-evaporated gold films. Ellipsometry measurements revealed that up to three layers could be assembled on gold in a 1 mM *n*-hexane solution of *p*-XDT while only one monolayer formed in either methanol or ethanol solution. Although the exact causes were uncertain, such a difference in behavior seemed to have nothing to do with the oxygen species present in ethanol or methanol solution.

The different adsorbate structure of *p*-XDT on gold and silver observed in this work is comparable to that of other dithiols investigated so far.[12−19] At the moment, the detailed origin of the different adsorption characteristics is not certain. Molecular mechanics calculations would be helpful for a better understanding of such a difference. Our previous molecular mechanics calculation have demonstrated that even the SAMs of benzene thiolate and benzyl mercaptide can have different structures on Au(111).[40] Since the theoretical work on monothiols such as HS and CH_3S by Sellers et al.[41] cannot be directly applied to the case of dithiols, it will also be worthwhile to perform a separate ab initio quantum mechanical calculation to clarify the different adsorbate structures of dithiols on gold and silver. Our future work will be advanced toward such directions.

Acknowledgment. This work was supported by the Korea Science and Engineering Foundation through the Center for Molecular Catalysis at Seoul National University (SNU) and by the Korea Research Foundation through the Research Institute for Basic Sciences at SNU.

References and Notes

(1) Ulman, A. *An introduction to ultrathin organic films from Langmuir−Blodgett to self-assembly*; Academic Press: San Diego, CA, 1991.

(2) Swalen, J. D.; Allara, D. L.; Andrade, J. D.; Chandross, E. A.; Garoff, S.; Israelachvili, J.; MaCarthy, T. J.; Murray, R.; Pease, R. F.; Rabolt, J. F.; Wynne, K. J.; Yu, H. *Langmuir* **1987**, *3*, 932.

(3) Ulman, A., Ed. *Thin Films*; Academic Press: San Diego, CA, 1995; Vol. 20.

(4) Laibinis, P. E.; Whitesides, G. M.; Allara, D. L.; Tao, Y.-T.; Parikh, A. N.; Nuzzo, R. G. *J. Am. Chem. Soc.* **1991**, *113*, 7152.

(5) Nuzzo, R. G.; Zegarski, B. R.; Dubois, L. H. *J. Am. Chem. Soc.* **1987**, *109*, 733.

(6) Joo, T. H.; Kim, K.; Kim, M. S. *J. Mol. Struct.* **1987**, *162*, 191.

(7) Kwon, C. K.; Kim, K.; Kim, M. S. *J. Mol. Struct.* **1989**, *197*, 171.

(8) Chidsey, C. E. D. *Science* **1991**, *251*, 919.

(9) Bryant, M. A.; Pemberton, J. E. *J. Am. Chem. Soc.* **1991**, *113*, 8284.

(10) Alves, C. A.; Smith, E. L.; Porter, M. D. *J. Am. Chem. Soc.* **1992**, *114*, 1222.

(11) Tour, J. M.; Jones, L.; Pearson, D. L.; Lamba, J. J. S.; Burgin, T. P.; Whitesides, G. M.; Allara, D. L.; Prikh, A. N.; Atre, S. V. *J. Am. Chem. Soc.* **1995**, *117*, 9529.

(12) Reed, M. A.; Zhou, C.; Muller, C. J.; Burgin, T. P.; Tour, J. M. *Science* **1997**, *278*, 252.

(13) Kohli, P.; Taylor, K. K.; Harris, J. J.; Blanchard, G. J. *J. Am. Chem. Soc.* **1998**, *120*, 11962.

(14) Murty, K. V. G. K.; Venkataramanan, M.; Pradeep, T. *Langmuir* **1998**, *14*, 5446.

(15) Rieley, H.; Kendall, C. K.; Zemicael, F. W.; Smith, T. L.; Yang, S. *Langmuir* **1998**, *14*, 5147.

(16) Nakanishi, T.; Ohtani, B.; Uosaki, K. *J. Phys. Chem. B* **1998**, *102*, 1571.

(17) Lee, T. G.; Kim, K.; Kim, M. S. *J. Phys. Chem.* **1991**, *95*, 9950.

(18) Kwon, C. K.; Kim, K.; Kim, M. S.; Lee, Y. S. *J. Mol. Struct.* **1989**, *197*, 171.

(19) Cho, S. H.; Han, H. S.; Jang, D.-J.; Kim, K.; Kim, M. S. *J. Phys. Chem.* **1995**, *99*, 10594.

(20) Chang, R. K., Furtak, T. E., Eds. *Surface Enhanced Raman Scattering*; Plenum Press: New York, 1982.

(21) Moskovits, M. *Rev. Mod. Phys.* **1985**, *57*, 783.

(22) Chase, B.; Parkinson, B. *J. Phys. Chem.* **1991**, *95*, 7810.

(23) Joo, T. H.; Kim, K.; Kim, M. S. *Chem. Phys. Lett.* **1984**, *112*, 65.

(24) Lee, P. C.; Meisel, D. *J. Phys. Chem.* **1982**, *86*, 3391.

(25) Gao, X.; Davies, J. P.; Weaver, M. J. *J. Phys. Chem.* **1990**, *94*, 6858.

(26) The concentration of *p*-XDT required for the monolayer coverage was calculated by the following scheme. Since the average diameter of a colloidal particle is 10 nm, its mean surface area and volume are estimated to be 310 nm^2 and 520 nm^3, respectively. Assuming that each ion of *p*-XDT^{2-} occupies an area of 0.58 nm^2 with a flat orientation on silver, the mean surface area of each colloidal particle, 310 nm^2, should correspond to that occupied by 534 *p*-XDT^{2-}. On the other hand, considering that the atomic radius of silver is 0.1445 nm,[27] the volume of each colloidal particle, 520 nm^3, should correspond to that of 4.1×10^4 Ag atoms. Since the colloidal sol was prepared with a 1×10^{-3} M $AgNO_3$ solution, the concentration of the final prepared colloidal particles should then be 6.1×10^{-9} M. The concentration of *p*-XDT required to cover all the colloidal silver particles is accordingly estimated to be 3.3×10^{-6} M, i.e., (534)(6.1×10^{-9}) M.

(27) Chidsey, C. E. D.; Loiacono, D. N.; Sleator, T.; Nakahara, S. *Surf. Sci.* **1988**, *200*, 45.

(28) The same calculation scheme as that in ref 26 is used. The only differences are that the average diameter of a gold colloidal particle is 50 nm, the atomic radius of gold is 0.144 25 nm,[27] the gold sol is prepared using a 1.3×10^{-3} M $KAuCl_4$ solution, and each *p*-XDT^{1-} ion is assumed to occupy an area of 0.217 nm^2 with a vertical orientation on gold.

(29) Cook, J. C.; Cuypers, C. M. P.; Kip, B. J.; Meier, R. J.; Koglin, E. *J. Raman Spectrosc.* **1993**, *24*, 609.

(30) Weitz, D. A.; Oliveria, M. *Phys. Rev. Lett.* **1984**, *52*, 1433.

(31) Moskovits, M.; Suh, J. S. *J. Am. Chem. Soc.* **1986**, *108*, 4711.

(32) Creighton, J. A. *Surf. Sci.* **1983**, *124*, 209.

(33) Moskovits, M. *J. Chem. Phys.* **1982**, *77*, 4408.

(34) Porter, M. D.; Bright, T. B.; Allara, D. L.; Chidsey, C. E. D. *J. Am. Chem. Soc.* **1987**, *109*, 3559.

(35) Bryant, M. A.; Pemberton, J. E. *J. Am. Chem. Soc.* **1991**, *113*, 3629.

(36) Bryant, M. A.; Pemberton, J. E. *J. Am. Chem. Soc.* **1991**, *113*, 8284.

(37) Kim, C. H.; Han, S. W.; Ha, T. H.; Kim, K. *Langmuir*, submitted.

(38) Bain, C. D.; Troughton, E. B.; Tao, Y.-T.; Evall, J.; Whitesides, G. M.; Nuzzo, R. G. *J. Am. Chem. Soc.* **1989**, *111*, 321.

(39) Tao, Y.-T.; Wu, C.-C.; Eu, J.-Y.; Lin, W.-L.; Wu, K.-C.; Chen, C.-H. *Langmuir* **1997**, *13*, 4018.

(40) Jung, H. H.; Won, Y. D.; Shin, S.; Kim, K. *Langmuir* **1999**, *15*, 1147.

(41) Sellers, H.; Ulman, A.; Shnidman, Y.; Eilers, J. E. *J. Am. Chem. Soc.* **1993**, *115*, 9389.